Helical single-lamellar crystals thermotropically formed in a synthetic nonracemic chiral main-chain polyester

Christopher Y. Li
The Maurice Morton Institute and Department of Polymer Science, The University of Akron, Akron, Ohio 44325-3909

Donghang Yan
Polymer Physics Laboratory, Changchun Institute of Applied Chemistry, Chinese Academy of Sciences, Changchun, Jilin 130022, China

Stephen Z. D. Cheng,* Feng Bai, Jason J. Ge, and Bret H. Calhoun
The Maurice Morton Institute and Department of Polymer Science, The University of Akron, Akron, Ohio 44325-3909

Tianbai He
Polymer Physics Laboratory, Changchun Institute of Applied Chemistry, Chinese Academy of Sciences, Changchun, Jilin 130022, China

Liang-Chy Chien
Liquid Crystal Institute, Kent State University, Kent, Ohio 44010-0001

Frank W. Harris
The Maurice Morton Institute and Department of Polymer Science, The University of Akron, Akron, Ohio 44325-3909

Bernard Lotz
Institute Charles Sadron, 6 Rue Boussingault, Strasbourg 67083, France
(Received 25 March 1999)

Phase structures and transformation mechanisms of nonracemic chiral biological and synthetic polymers are fundamentally important topics in understanding their macroscopic responses in different environments. It has been known for many years that helical structures and morphologies can exist in low-ordered chiral liquid crystalline (LC) phases. However, when the chiral liquid crystals form highly ordered smectic liquid crystal phases, the helical morphology is suppressed due to the crystallization process. A double-twisted morphology has been observed in many liquid crystalline biopolymers such as dinoflaggellate chromosomes (in *Prorocentrum micans*) in an *in vivo* arrangement. Helical crystals grown from solution have been reported in the case of *Bombyx mori* silk fibroin crystals having the β modification. This study describes a synthetic nonracemic chiral main-chain LC polyester that is able to thermotropically form helical single lamellar crystals. Flat single lamellar crystals can also be observed under the same crystallization condition. Moreover, flat and helical lamellae can coexist in one single lamellar crystal, within which one form can smoothly transform to the other. Both of these crystals possess the same structure, although translational symmetry is broken in the helical crystals. The polymer chain folding direction in both flat and helical lamellar crystals is determined to be identical, and it is always along the long axis of the lamellae. This finding provides an opportunity to study the chirality effect on phase structure, morphology, and transformation in condensed states of chiral materials. [S0163-1829(99)01042-5]

I. INTRODUCTION

Natural and synthetic nonracemic chiral materials play important roles in developing modern science and technology. Knowledge of their phase structures and transformation behaviors is critical to design and engineer molecular and supramolecular packings to achieve macroscopic properties desired for specific applications. In the past, two connected research areas have been active in attempting to understand the effect of chirality on phase behaviors in condensed matter physics. The first area is in biological polymers, while the second is in chiral liquid crystals (LC's).

In considering biological polymers such as globular proteins and silk fibroin, all of which are configurationally chiral (primary structure), the general understanding is that both the α-helix and the β-pleated sheet are two common secondary classes of structures that construct the tertiary structures of these biological polymers. The β-pleated sheet consists of hydrogen bonding within the sheets, as first proposed by Pauling and his colleagues and confirmed using wide angle x-ray diffraction.[1,2] It was found later that the neighboring chiral chain packing of these β sheets in some of the globular proteins are twisted and deviate from a 2_1 symmetry along the long axis of the sheet. Based on the local conformational calculations, the twisted sheets show a lower free energy than those possessing the 2_1 symmetry.[3] When these twisted β sheets pack together, another twist, which is perpendicular to the β sheet's helical axis is constructed and, therefore, a double-twisted helical tertiary structure can be formed. A direct morphological observation of a similar type of helical

structure has been reported in dinoflagellate chromosomes (in *Prorocentrum micans*) in an *in vivo* arrangement.[4] It has also been found that *Bombyx mori* silk fibroin can grow a helical lamellar crystal of the β modification under solution crystallization conditions.[5]

In the past two decades, the availability of synthetic nonracemic chiral substances in LC's has led to the discovery of structures and related phase behaviors over a broad research area, including ferroelectric, ferrielectric, antiferroelectric, and other LC's.[6] Helical structures in molecular and supramolecular levels induced by chirality are known in low-ordered LC phases, such as in cholesteric (Ch) phases,[7–9] blue phases,[10,11] smectic C*(S_C^*) phases,[12] and twisted grain boundary (TGB) phases.[13–17] The interesting feature in these phases is that they contain a supramolecular helical morphology, which is an intrinsic characteristic of the nonracemic chiral LC's. In a Ch phase, the long axes of the molecules lie within each layer and are always perpendicular to the helical axis. In a S_C^* phase, the smectic layer normal is parallel to the helical axis, while the molecules keep the same angle yet rotate in equal radian with respect to the helical axis. In TGB phases, on the other hand, the smectic layer normal is always perpendicular to the helical axis. Being well developed in low-ordered chiral LC phases, helical morphology, however, has not been observed in the highly ordered LC phases, such as smectic crystal J^*, G^*, H^*, and K^* phases. It is believed that the helical morphology is suppressed by the crystallization interactions.[6]

Another apparently related issue of the twisted lamellar crystals is in the banded spherulitic morphology of synthetic nonchiral polyethylene (PE) and other polymers.[18,19] Both nonracemic chiral enantiomorphism and chain tilt in lamellar crystals may induce twisting.[18,20] Chiral poly(epichlorohydrin)s with both antimorphs in their spherulitic formations have also been reported.[21,22] It has been found that the configurational chirality (primary structure) determines the sense of crystal rotation underlying the banded structure of spherulites.[22] Although the twist in polymer crystals has been used to explain the optical behavior of the banded structure of spherulites, helical single crystals have not been observed. The reason may be associated with the fact that a nonracemic chiral helical conformation (secondary structure) may not be spontaneously extended to a nonracemic chiral helical morphology (tertiary structure) since the morphology is determined by molecular packing.

Our objective is to enhance the rigidity of the nonracemic chiral polymers to strengthen the chirality in order to achieve highly ordered chiral helical morphology. In this publication, we report our first observation on both flat and helical single lamellar crystals formed thermotropically in a synthetic nonracemic chiral main-chain polyester. The crystal structure and chain-folding direction are determined. Possible formation mechanisms are discussed.

II. EXPERIMENTAL SECTION

A. Materials and sample preparation

The polymer reported here was synthesized from (R)-(-)-4'-{ω-[2-(*p*-hydroxy-*o*-nitrophenyloxy)-1-propyloxy]-1-nonyloxy}-4-biphenyl carboxylic acid. The number of methylene units is nine, and this nonracemic chiral polymer is abbreviated as PET(R*)-9.[23] In brief, the monomer was synthesized starting from ethyl-(S)-(−) lactate utilizing the Finklestein reaction, alkylation, Baeyer-Villiger oxidation, Mitsunobu reaction, and then hydrolysis of the corresponding precursor afforded the desired monomer. The polymerization was directly conducted from this monomer via an A-B−type condensation using the catalyst 4-(dimethylamino) pyridinium 4-toluenesulfonate under mild conditions. The polymer chemical structure is shown in Fig. 1. Note that in this polyester, there is no hydrogen bonding involved in the molecular packing. The polymer possesses right-hand chiral centers (*) along the main-chain backbone. The specific rotation of the monomer is $[\alpha]_D = -28.5°$. The molecular weight of PET(R*)-9 is around 16,000 g/mol with a polydispersity of approximately 2, as measured by gel permeation chromatography based on polystyrene standards.

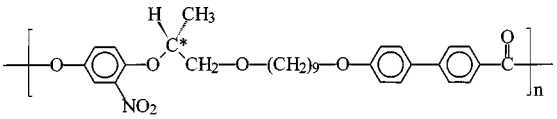

FIG. 1. Polymer PET (R*)-9 chemical structure.

Polymer thin films (with a thickness of around 50–100 nm) were prepared via a solution casting method from a 0.05% tetrahydrofuran solution on carbon-coated glass surfaces. After the solvent was evaporated, the films were heated in a Mettler FP-90 heating stage to above its highest endothermic transition temperature as measured by differential scanning calorimetry. The films were subsequently quenched to preset temperatures and held isothermally for various times ranging from several minutes to a few days. The samples were then quenched in liquid nitrogen and allowed to return to room temperature, which is below the glass transition temperature of the polymer ($T_g = 37\,°C$).

B. Equipment and experiments

The thin film samples prepared for transmission electron microscopy (TEM) observations were first examined under both polarized light and phase-contrast microscopes before they were shadowed by Pt and coated with carbon for TEM observations (this is because the size of the single crystals lies in a range of a few μm to over 50 μm). The TEM experiments were carried out in a JEOL (1200 EX II) TEM using an accelerating voltage of 120 kV. Electron diffraction (ED) patterns of the samples having different zones were also obtained using a TEM tilting stage ($\pm 60°$) in order to determine the three-dimensional crystalline unit cells. Calibration of the ED spacing was done using TlCl in a *d*-spacing range smaller than 0.384 nm, which is the largest spacing for TlCl. Spacing values larger than 0.384 nm were calibrated by doubling the *d* spacing of those reflections based on their first-order reflections.

In order to examine the chain-folding direction, low molecular weight polyethylene (PE) decoration was utilized following a procedure previously reported.[24,25] In brief, a linear PE fraction obtained from Phillips Petroleum Company was used as the decoration material. Its number-average molecular weight was 17,300 g/mol and polydispersity was 1.11. During the decoration, an optimal 10 cm distance between the sample and the basket was chosen in the vacuum evapo-

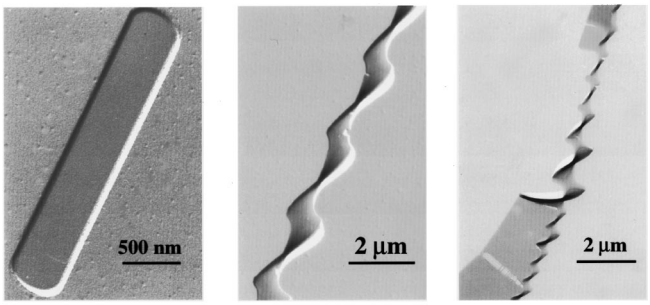

FIG. 2. A flat lamellar crystal grown from the melt at 160 °C for 24 h and observed under TEM (a). A twisted helical lamellar crystal grown from the melt at 145 °C for 24 h and observed under TEM (b). A lamellar crystal grown from the melt at 145 °C for 24 h showing the coexistence of flat and helical crystals, the lower left side showing the microfibers in the crack of the crystal (c).

rator where PE was degraded and evaporated. The samples were then treated following the standard procedure as described previously.[24,25]

III. RESULTS AND DISCUSSION

A. Flat and twisted helical lamellar crystals

PET(R*)-9 has demonstrated that upon cooling, high-temperature chiral smectic LC phase transitions occur in the vicinity of 189 °C, followed by further ordering processes and crystallization above the T_g.[23,26] Figure 2(a) shows a TEM micrograph of a flat lamellar crystal grown via quenching from the isotropic melt to 160 °C and isothermally crystallized for one day. An elongated shape of the crystal can be found with a large aspect ratio between the long and short lamellar axes. By using the metal shadowing technique, the lamellar thickness is found to be around 20 nm.

Figure 2(b) shows a twisted single helical lamellar crystal of a PET(R*)-9 sample observed in TEM. The sample was isothermally crystallized at 145 °C for one day. Based on the metal shadowing, one can estimate the lamellar thickness to be 15 nm. The crystal surfaces observed at this resolution appear smooth with a continuous and periodically changing curvature. In all of our observations, the twisted helix is always right-handed (note that the chiral center is right-handed) with a pitch length of approximately 1.5–5.0 μm, depending upon crystallization temperatures (T_cs). A higher T_c leads to a longer pitch length. This indicates that with increasing T_c, the chirality effect on the twisted molecular packing decreases and the parallel chain packing becomes increasingly dominant. The correspondence of two different structural hierarchies, the primary configurational chirality (chiral center) and tertiary morphological chirality (helical lamella), depends upon the secondary conformational chirality, since this secondary structure determines the molecular packing scheme. Computer simulations of the chain conformation and packing are necessary to understand this correspondence.

It is intriguing that in our observations both flat and helical lamellar crystals can be found under the same crystallization condition. The first impression is that these two crystals may grow based on film thickness restrictions. A relatively thin film develops the flat crystals and a relatively thick film provides the material and space for the helical crystal growth. However, careful examination indicates that this geometrical factor is not the only reason, since multiple-layer flat lamellar crystals can also form even in a quite thick film. Furthermore, at most of the T_cs the flat and helical crystals may also be molecularly joined together as shown in Fig. 2(c), suggesting that these crystals can be converted from one to another. This coexistence can be either along the long lamellar axis or along the short lamellar axis to form the side-by-side flat and helical crystal [the lower left of Fig. 2(c)]. The conversion appears to occur on a scale of molecular packing. This observation suggests that the free energies of forming the flat and helical molecular packing may be comparable, and therefore, both of the morphologies can be observed. Detailed free-energy calculations in the crystal structures are required in order to quantitatively analyze this speculation.

B. Determination of the flat lamellar crystal lattice

A [001] zone ED pattern of the flat lamellar crystal of Fig. 2(a) is shown in Fig. 3(a). The ED pattern represents an a^*b^* two-dimensional lattice with the b^* axis parallel to the long axis of the lamellar crystal. The basic unit-cell dimensions can be determined as $a = 1.07$ nm and $b = 0.48$ nm. The c-axis dimension can be obtained through the ED patterns of different zones using the tilting stage, also shown in Fig. 4. It is evident that $\pm 14°$, $\pm 18°$, and $\pm 22°$ rotations along the a^* axis lead to the $[0\bar{3}1]$, $[0\bar{4}1]$, and $[0\bar{5}1]$ zones, and similarly, $\pm 5°$, $\pm 19°$, and $\pm 35°$ rotations along the b^* axis lead to the $[\bar{1}02]$, $[\bar{2}01]$, and $[\bar{4}01]$. Hence, the c dimension can be calculated to be 5.96 nm. This value represents the repeating distance of a 2_1-helical conformation along the chain direction in the crystals.

One can observe that in the [001] zone ED pattern [Fig. 3(a)] the (h10) layer intensities are strong. However, there is another parallel diffraction layer [the arrow in Fig. 3(a)] above the (h10) layer. The distance between this layer and the (h10) layer is one third of that between the (h00) and the (h10) layers. Comparing the (h10) layer with the (h00) layer

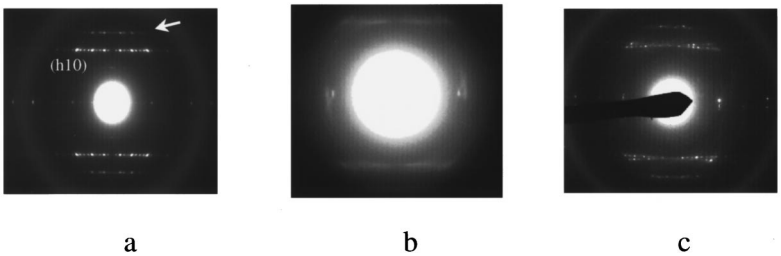

FIG. 3. ED patterns taken from the flat lamellar crystal shown in Fig. 2(a) (a); the helical lamellar crystals shown in Fig. 2(b) (b); and occasionally, a sharp ED pattern taken from helical lamellar crystals can be obtained (c).

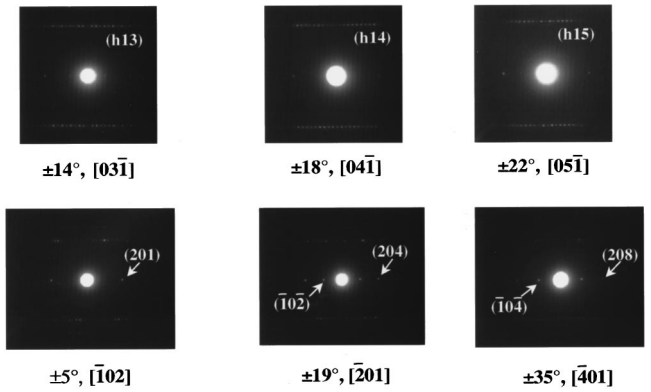

FIG. 4. Set of ED patterns without and with rotations of the a^*- and b^* axes at different angles obtained from a flat lamellar crystal as shown in Fig. 2(a).

in the ED pattern having the [001] zone in Fig. 3(a), the diffractions of the (h10) layer are five times denser than that of the a^* axis of the basic unit given by the (h00) layer diffractions. This may indicate that commensurate structures exist and they are superimposed on the basic unit cell along the a axis with a periodicity five times larger than the a dimension of the unit cell.

Figure 5 shows an ED pattern obtained from a sheared sample, which is along the [010] zone. This is consistent with the previous unit-cell symmetry and dimension determinations, and more importantly, a five-times larger unit cell along the a^* axis cannot be observed in this ED pattern, suggesting that the commensurate structures are not essential in the lattice of the a^*c^* plane and may be destroyed by mechanical shearing.

C. Determination of helical lamellar crystal lattice

The ED pattern obtained from the circular area of the helical lamellar crystal [Fig. 2(c)] is shown in Fig. 3(b). The diffraction pattern is fairly diffused, since the crystal lattice is continuously twisted in the helical lamellar crystal. It is difficult to calculate the crystal structure based on this diffused ED pattern. On some occasions, however, sharp ED patterns can also be obtained in the twisted helical lamellar

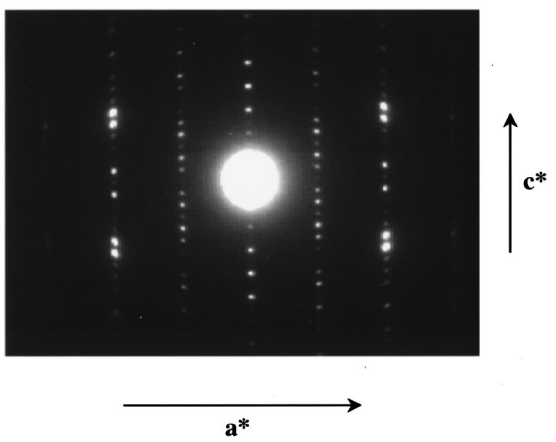

FIG. 5. A [010] zone single crystal ED pattern obtained from a sheared sample. Note that the commensurate structure is not found in this pattern.

crystals as shown in Fig. 3(c) depending on the pitch length and the orientation of the chains in the crystal with respect to the electron beam. It is evident that the helical lamellar crystals possess the same crystal structure as the flat ones by comparing Fig. 3(c) with Fig. 3(a) which possesses the [001] zone. In particular, the ED result in Fig. 3(c) gives two superimposed ED patterns with a rotation angle of 6° along the substrate normal. The reciprocal lattice calculation shows that these two ED patterns possess the $[13\bar{1}]$ and $[36\bar{2}]$ zones, respectively, suggesting that they arise from two different orientations of the same crystal lattice. It should be noted that within the lattice of a completely flat crystal with the chain orientation parallel to the lamellar surface normal, the $[13\bar{1}]$ and $[36\bar{2}]$ zones should be 7.88° apart from each other. However, in Fig. 3(c) both zones are aligned with the electron beam direction. As a result, these two orientations deviate from those in the lattice of the flat crystals, providing a characteristic of the twisted helical crystals. Furthermore, the 6° rotation between these two ED patterns demonstrates that there is a 6° angle between the intersections of the two b^*c^* planes with the substrate surface. The ED pattern in Fig. 3(c) thus suggests that the chain molecules in this lamellar crystal are possibly double twisted, although this experimental observation alone is not sufficient to uniquely prove this arrangement. Further experiments such as dark field TEM studies are necessary.

It is interesting that the flat and helical lamellar crystals possess the same crystal structures. Crystallographically, it is impossible to use translation symmetry to transfer a smoothly twisted (curved) lattice into a flat (linear) one in a three-dimensional space. Therefore, the Euclidean symmetry groups represented in a linear coordination must undergo a transformation to a curved coordination in the three-dimensional space. From a structural point of view, defects must play a role. This may be formed in two possible ways.

First, the twisted helical crystals may be constructed through a continuous but slight rotation of neighboring packed molecules in the crystal unit cells (a continuous model). The rotational angle between adjacent layers along the long helical axis can be roughly estimated by calculating the ratio between the pitch length and the thickness of one molecular layer. The pitch length of PET(R*)-9 ranges from 1.5 to 5.0 μm with $b = 0.48$ nm. This approximation leads to an angle between 0.02° and 0.06° per molecular layer along the long helical axis depending upon the T_cs.

The second possible way involves the crystal being divided into small, discrete domains with a certain size, and within each of these domains the flat crystal exists. The boundary between two domains acts as defects (a discrete model). These defect boundaries must be small enough in size in order to maintain a relatively low overall free energy and still retain a stable helical crystal. Therefore, the overall twisted structure consists of a number of flat domains connected by defects.[27,28] This has been observed in low-ordered LC's where this type of structure is necessary to construct twisted morphology and the defects are related to the disclinations (for example, the TGB phases[13–17]). In the crystal case, it is the dislocations to which the defects are attributed. It can be expected that when the domain size in the discrete model decreases towards the size of molecular layer, the continuous rotation may gradually replace the defect boundaries and, therefore, the discrete model will eventually become

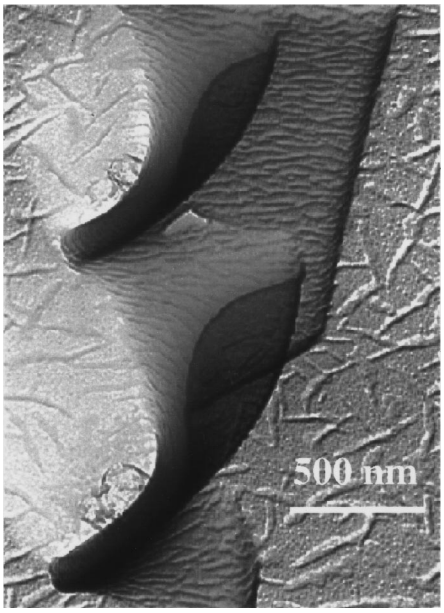

FIG. 6. Low molecular weight PE crystal decorated PET*-9 flat lamellar crystal and the twisted lamellar crystal observed under TEM. Note that the helical lamellar crystal grows on the top of the flat one. The *c* axis of the PE crystals (which is perpendicular to the needlelike PE crystals) is parallel to the long axis of both the lamellar crystals. The crystallization conditions are the same as in Figure 2(b).

indistinguishable from the continuous one. We believe that these helical lamellar crystals follow the first twisting mechanism since, based on our observations, the twist surfaces seem to be smooth and continuous down to a size resolution of 5 nm in the TEM observations.

D. Chain folding directions in both types of lamellar crystals

The question pertaining to the mechanism of the helical crystal formation of the long chain isochiral molecules is also essential to resolve. One must first know if the chain molecules are folded, and if so, what the folding direction is. The low molecular weight PE decoration method was utilized[23,24] in our experiments. Figure 6 shows the PE-decorated lamellar crystal. The crystal consists of both flat and helical parts. It is clear that the elongated direction of the PE crystal rods on the flat part of the crystal is perpendicular to the *b* axis (the crystal long axis) and the *c* axis of the PE crystals is parallel to the *b* axis of the crystal. Therefore, the chain-folding direction is along the *b* axis (the crystal long axis). On the other hand, the helical part of the PE-decorated crystal in Fig. 6 also shows that the elongated direction of the PE crystals is more or less perpendicular to the helical long axis. Therefore, the *c* axis of the elongated PE crystals should be globally parallel to the helical axis. One can thus conclude that in the helical lamellar crystals, the chain-folding direction is also along the long helical axis. This indicates that the helical structure does not fundamentally change the molecular chain-folding behavior. These observations are similar to the cases of β sheets in globular proteins and other biological polymers in which the protein folding is along the advancing direction (the long helical axis direction) of the sheets. Moreover, in Fig. 6, the decorated PE crystal shows that both the top and bottom of the helical crystal surfaces exhibit identical folding behavior.

The conclusion of the chain-folding direction in the decoration experiment can also be indirectly supported in Fig. 2(c). When a crack develops across the direction perpendicular to the long lamellar crystal axis as shown in Fig. 2(c), microfibers along the long crystal axis can be observed. This indicates that during the crack formation the chain molecules are pulled out from the crystal to recrystallize into the microfiber form due to the molecular continuity. Note that the microfiber can only be observed when the chain-folding direction is not parallel to the crack direction.

IV. CONCLUSION

From this study of flat and helical lamellar crystals, it has been found that, with the exception of the crystallization from the thermotropically less ordered LC state, this nonracemic chiral main-chain polyester has exhibited remarkable similarity to biological polymers in both phase formation and morphology. Two important observations should be emphasized. First, the single helical lamellar crystals possess a regular orthorhombic unit-cell structure, identical to that of the flat lamellar crystals. Second, the molecular chain folding is along the long lamellar axis in both of the flat and helical lamellar crystals, indicating that the chain folding is directly towards the less-ordered LC state. These observations are essential for understanding and further discussing the formation mechanisms of both the flat and helical lamellar crystals in this chiral polymer.

ACKNOWLEDGMENTS

We are grateful for the funding from NSF (DMR-9617030) and NSF ALCOM Science and Technology Center (DMR-8920147). S.Z.D.C., D.Y., and T.H. also thank the cooperative research grants from Chinese NNSF (29474143 and 29674030). Thoughtful and in-depth discussions with Dr. F. Khoury regarding this topic are greatly acknowledged.

*Author to whom correspondence should be addressed. Electronic address: cheng@polymer.uakron.edu

[1] L. Pauling, R. B. Corey, and H. R. Branson, Proc. Natl. Acad. Sci. USA **37**, 205 (1951).
[2] F. Lucas, J. T. B. Shaw, and S. G. Smith, Biochem. J. **66**, 468 (1957).
[3] C. Chothia, J. Mol. Biol. **75**, 295 (1973).
[4] F. Livolant and Y. Bouligand, Chromosoma **80**, 97 (1980).
[5] J. Magoshi, J. Mol. Biol. **156**, 345 (1982).
[6] J. W. Goodby, A. J. Slaney, C. J. Booth, I. Nishiyama, J. D. Vuijk, P. Styring, and K. J. Toyne, Mol. Cryst. Liq. Cryst. Sci. Technol., Sect. A **243**, 231 (1994).
[7] G. Friedel, Ann. Phys. (Paris) **18**, 273 (1992).
[8] A. Saupe, Angew. Chem. Int. Ed. Engl. **7**, 97 (1968).
[9] A. D. Buckingham, G. P. Ceasar, and M. B. Dunn, Chem. Phys. Lett. **3**, 540 (1969).
[10] A. Saupe, Mol. Cryst. Liq. Cryst. **7**, 59 (1969).
[11] S. Meiboom, J. P. Sethna, P. W. Anderson, and W. F. Brinkman,

Phys. Rev. Lett. **46**, 1216 (1981).
[12] W. Helfrich and C. S. Oh, Mol. Cryst. Liq. Cryst. **14**, 289 (1971).
[13] P. G. de Gennes, Solid State Commun. **10**, 753 (1972).
[14] S. R. Renn and T. C. Lubensky, Phys. Rev. A **38**, 2132 (1988).
[15] T. C. Lubensky and S. R. Renn, Phys. Rev. A **41**, 4392 (1990).
[16] J. W. Goodby, M. A. Waugh, S. M. Stein, E. Chin, R. Pindak, and J. S. Patel, J. Am. Chem. Soc. **111**, 8119 (1989).
[17] J. W. Goodby, M. A. Waugh, S. M. Stein, E. Chin, R. Pindak, and J. S. Patel, Nature (London) **337**, 449 (1989).
[18] For a recent summary, see H. D. Keith and F. Padden Jr., Macromolecules **29**, 7776 (1996).
[19] R. M. Briber and F. A. Khoury, J. Polym. Sci., Polym. Phys. Ed. **31**, 1253 (1993).
[20] H. D. Keith, F. Padden Jr., B. Lotz, and J. C. Wittmann, Macromolecules **22**, 2230 (1989).
[21] K. L. Singfield and G. R. Brown, Macromolecules **28**, 8006 (1995).
[22] K. L. Singfield, J. K. Hobbs, and A. Keller, J. Cryst. Growth **183**, 683 (1998).
[23] F. Bai, L. C. Chien, C. Y. Li, S. Z. D. Cheng, and R. Petschek, Chem. Mater. **11**, 1666 (1999).
[24] J. C. Wittmann and B. Lotz, Makromol. Chem., Rapid Commun. **3**, 733 (1982).
[25] J. C. Wittmann and B. Lotz, J. Polym. Sci., Polym. Phys. Ed. **23**, 205 (1985).
[26] C. Y. Li, D. Yan, S. Z. D. Cheng, F. Bai, T. He, L. C. Chien, F. W. Harris, and B. Lotz, Macromolecules **32**, 524 (1999).
[27] M. Kleman, Adv. Phys. **38**, 605 (1989).
[28] R. D. Kamien and D. R. Nelson, Phys. Rev. E **53**, 650 (1996).